Dynamic pressure enhancements as a cause of large-scale stormtime substorms

L. R. Lyons,[1] D.-Y. Lee,[2] S. Zou,[1] C.-P. Wang,[1] J. U. Kozyra,[3] J. M. Weygand,[4] and S. B. Mende[5]

Received 6 November 2007; revised 31 January 2008; accepted 31 March 2008; published 13 August 2008.

[1] Intense substorm disturbances, which typically have an unusually broad auroral enhancement, occur in association with magnetic storms. We have investigated the cause of these intense and broad disturbances using interplanetary observations, global auroral images from the WIC imager on the IMAGE spacecraft, geosynchronous energetic particle observations, and mid/low-latitude dayside ground H observations for 28 large stormtime auroral disturbances. We find evidence that the magnetosphere was impacted by a substantial P_{dyn} increase at the onset of 19 of these disturbances. For disturbances with evidence of such an impact, we found that auroral brightenings extended over about twice as broad an MLT range as did the auroral brightening of disturbances that did not have evidence for a P_{dyn} increase at onset. We thus conclude that P_{dyn} increases at onset offer a feasible explanation for many of the larger-scale aurora disturbances that often occur during magnetic storms. Our results indicate that it is the combination of the global compression response to a P_{dyn} increase and the nightside substorm response that gives a much broader response for many stormtime disturbances than is seen from the substorm alone. We also found some indications that a substantially shorter than typical growth phase may be sufficient for there to be a triggered substorm onset if the preceding IMF $|B_y|$ or negative B_z, and/or a pressure increase at onset, is unusually large.

Citation: Lyons, L. R., D.-Y. Lee, S. Zou, C.-P. Wang, J. U. Kozyra, J. M. Weygand, and S. B. Mende (2008), Dynamic pressure enhancements as a cause of large-scale stormtime substorms, *J. Geophys. Res.*, *113*, A08215, doi:10.1029/2007JA012926.

1. Introduction

[2] Intense substorm disturbances having an unusually broad auroral disturbance occur during magnetic storms. There are varying numbers of such disturbances during storms. They can occur only once or twice, but occasionally several occur in succession every ~2–4 hours and are referred to as sawtooth events [e.g., *Reeves et al.*, 2002, 2004]. The cause of the unusually broad, intense disturbances has not yet been determined.

[3] Magnetic storms develop during periods of strongly southward interplanetary magnetic field (IMF), and we have recently found [*Lyons et al.*, 2005; *Lee et al.*, 2005] that a solar wind dynamic pressure P_{dyn} enhancement following strongly southward IMF conditions can cause a disturbance having fundamentally important differences from those under other conditions. P_{dyn} enhancements that do not follow strongly southward IMF conditions generally lead only to a global auroral brightening. These disturbances do not include a nightside substorm disturbance, and are far less intense than P_{dyn} disturbances under strongly southward IMF conditions, which have a substorm response in addition. Following strongly southward IMF conditions, a nightside substorm auroral brightening as well as compressive auroral brightening away from the substorm bulge region is seen near the time of onset. Auroral images suggest that, as the substorm bulge aurora expands in azimuth and the compressive auroral enhancement increases, the two auroral enhancements merge together leading to an auroral enhancement that is much broader than for typical substorms, covering ~10–15 hr of MLT. We also found that energetic particles at synchronous orbit and low-latitude H measurements show concurrent signatures of this two-mode (both compressional and substorm) response.

[4] Rigorous criteria for what P_{dyn} increases are sufficient to trigger a substorm have not yet been developed as a function of preceding conditions. However, the P_{dyn} trigger examples in *Lyons et al.* [2005] and *Lee et al.* [2005] suggest that P_{dyn} increases by the lesser of 50% or 3 nPa within 10 min and that remain elevated for 10 min following 1 hr of IMF B_z −8 nT are required. It has been demonstrated that northward turnings of the IMF also can trigger substorms [*Lyons et al.*, 1997; *Hsu and McPherron*,

[1]Department of Atmospheric and Oceanic Sciences, University of California, Los Angeles, Los Angeles, California, USA.
[2]Department of Astronomy and Space Science, Chungbuk National University, Chungbuk, South Korea.
[3]Space Physics Research Laboratory, University of Michigan, Ann Arbor, Michigan, USA.
[4]Department of Earth and Space Sciences, University of California, Los Angeles, Los Angeles, California, USA.
[5]Space Sciences Laboratory, University of California, Berkeley, California, USA.

0148-0227/08/2007JA012926

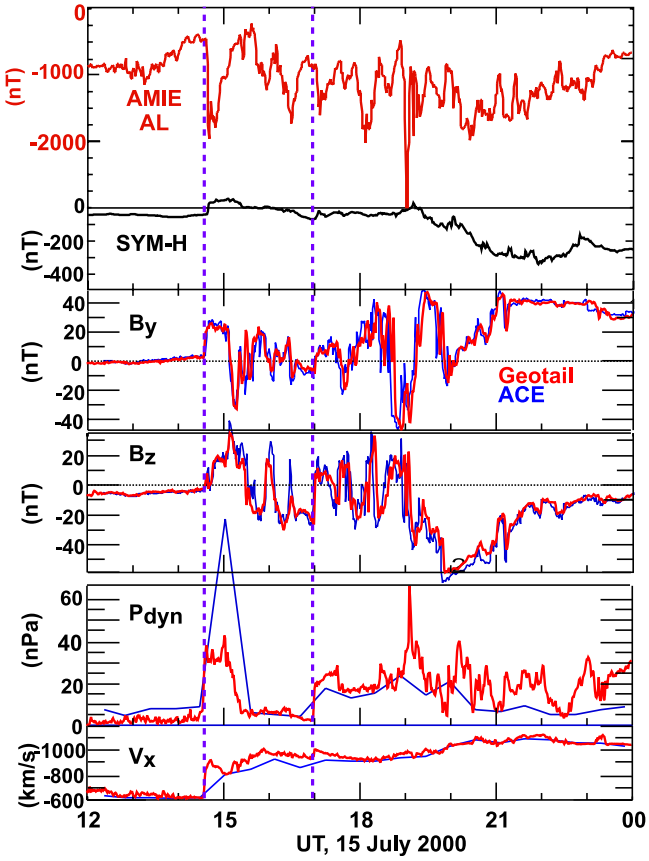

Figure 1. IMF and solar wind measurements, as well as the AL index obtained from the AMIE procedure and Sym-H, for 12–24 UT on 15 July 2000. Geotail data has been Weimer-mapped to X_{GSM} = 17 R_E directly in front of the magnetosphere, The ACE data have been linearly time-shifted to match the Geotail magnetic fields at ~15–17 UT, and the ACE re-analyzed low-time-resolution broad-energy-range plasma data has been used because the normal level 2 data is not available during this period. Vertical dashed lines indicate the times of the two disturbances discussed in the text.

2002], however they do not lead to the two-mode response unless accompanied by a P_{dyn} increase.

[5] This two-mode response is consistent with the concept proposed by *Elphinstone et al.* [1996] that disturbances in the auroral oval at any given time are composed of contributions from a variety of different magnetospheric processes in addition to substorms. These processes can act entirely independently of one another or be coupled. As described in *Lyons et al.* [2005], when acting independently substorms and dynamic pressure disturbances produce very different signatures in the auroral ionosphere. However, after preconditioning by an interval of strongly enhanced convection, the two processes can become coupled, and P_{dyn} disturbances can lead to substorms. The two processes combined then lead to unusually broad (in MLT) auroral disturbances.

[6] To date, no other specific type of disturbance has been shown to lead to such a broad and intense auroral activation, which motivates us to consider whether dynamic pressure impacts under strongly southward IMF conditions are responsible for the unusually large MLT-extent of some auroral disturbances during storms. To obtain a set of broad and intense disturbances during magnetic storms, we constructed a list of magnetic storms over the past several years that contained large auroral activations and a set of well-observed storms that have been characterized as sawtooth events. Sawtooth events are quasi-periodic large-amplitude geosynchronous particle injections that occur during moderate magnetic storms and are often unusually broad in MLT and include substorm auroral activations [*Henderson et al.*, 2006]. We use global auroral images from the Wideband Imaging Camera (WIC) on the IMAGE spacecraft, low-latitude ground magnetic field measurements, geosynchronous energetic particles, and solar wind data to evaluate whether individual disturbances have the signatures identified by *Lyons et al.* [2005] and *Lee et al.* [2005]. We find evidence that impact on the magnetosphere of solar wind pressure enhancements can lead to the large-scale auroral disturbances spanning a broad range in MLT that are observed under magnetic storm conditions.

2. Storms With Large Auroral Activations

[7] From the list of storms selected because of identified large-auroral activations, we chose to examine only large-scale disturbances for which global auroral images are available from WIC. Figure 1 shows IMF and solar wind measurements, as well as the AL index obtained from the assimilative mapping of ionospheric electrodynamics (AMIE) procedure [*Richmond*, 1992] and the Sym-H index, for 12–24 UT on 15 July 2000. (We show Sym-H because of its higher time resolution than Dst, as recommended by *Wanliss and Showalter* [2006].) Because of high particle backgrounds from strong and sustained solar particle events, the time resolution of ACE velocity and density measurements in the solar wind was degraded to ~30 minutes from 11:06 UT on July 14 to 01:33 UT on July 16 [*Smith et al.*, 2001]. The Geotail data, obtained in front of the magnetosphere (25, 9, −2 R_E GSM at 18 UT) are shown as mapped to X_{GSM} = 17 R_E using the *Weimer* [*Weimer et al.*, 2003; *Weimer*, 2004] technique. The ACE data have been linearly time-shifted to match the Geotail magnetic fields at ~15–17 UT. A storm sudden commencement occurred at 1438 UT due to a very large P_{dyn} increase after a prolonged period of moderately strong IMF Bz ~ −5 nT. This was followed by an intense storm main phase that initiated shortly after 19 UT. The sudden commencement P_{dyn} increase led to a large auroral disturbance seen by WIC. A second large P_{dyn} increase at ~1700 UT, following an approximately half-hour of strongly southward Bz ~ −20 nT, also led to a large auroral disturbance. Each of these disturbances was associated with a significant IMF northward turning, which even in the absence of an increase in P_{dyn} would be expected to trigger a nightside substorm disturbance [*Lyons et al.*, 1997], and with drops in AL to large negatives values (near ~1500 nT). There were two earlier northward turnings, one before and one after 16 UT, but these were not preceded by the >20–30 min growth-phase period prior that is normally required for an IMF northward turning to trigger a substorm.

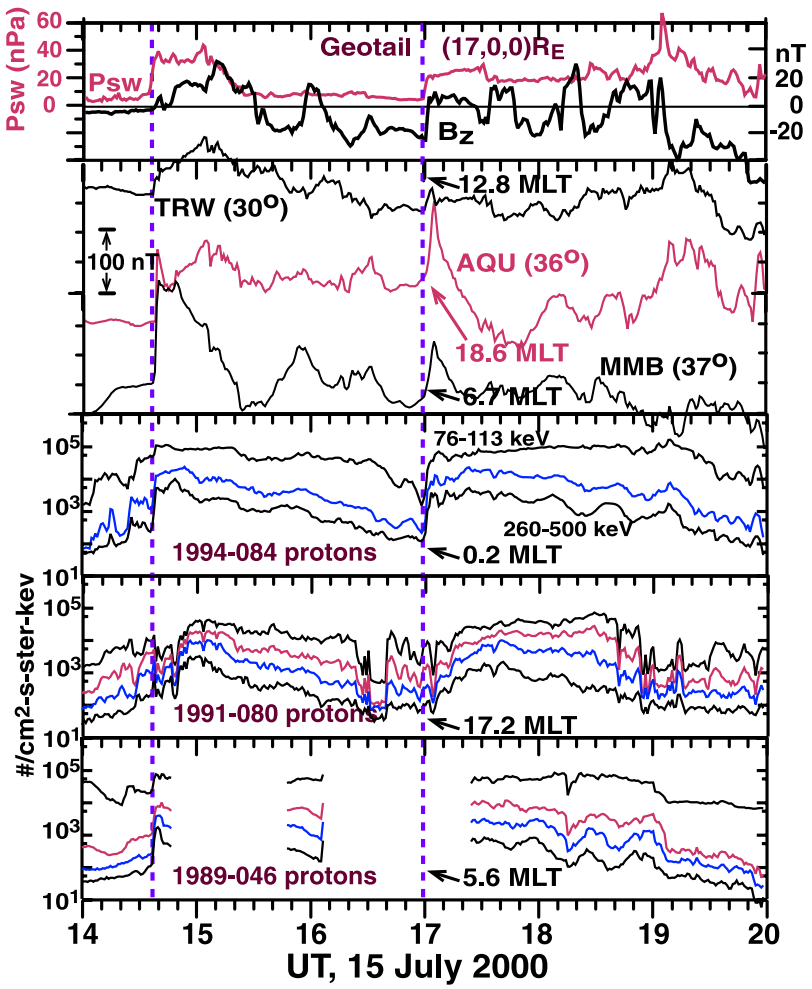

Figure 2. Mid-latitude ground H observations from three stations chosen to be near dawn, noon, and dusk and energetic proton fluxes from all available LANL spacecraft. The Weimer-mapped Geotail IMF and P_{dyn} observations from Figure 1 are repeated in the upper panel. Vertical dashed lines indicate the times of the two disturbances discussed in the text.

[8] The second panel from the top in Figure 2 shows mid-latitude ground H observations from three stations chosen to be near dawn, noon, and dusk. Abrupt increases at all three stations clearly identify the impact of each of the above P_{dyn} increases. The impacts occur just following the predicted arrivals of the Weimer-mapped P_{dyn} observations at 17 R_E upstream (repeated in the upper panel of Figure 2). Energetic proton fluxes from all available LANL spacecraft are also shown in Figure 2. The spacecraft closest to midnight, 1994–084, shows sharp dispersionless injections for each disturbance, which is the typical substorm signature. At nearly the same time, dispersionless responses are seen at the other spacecraft for which there is data. Such a global particle response is commonly associated with impacts of abrupt P_{dyn} increases [*Lee et al.*, 2005 and references therein].

[9] WIC images for each of the two disturbances are shown in the top two rows, respectively, of Figure 3. Successive 2 min images are shown for the times before, at, and after the first discernible auroral intensification, along with two later expansion phase images that show the subsequent auroral development. The images show the two-mode response for both pressure impacts. For the first P_{dyn} increase, a nightside substorm auroral brightening is seen near 21 MLT in the 1438 UT image, and for the second P_{dyn} increase, a nightside substorm auroral brightening is seen near 24 MLT in the 1701 UT image. For each event, brightening away from the substorm onset region, which is the expected direct result of magnetospheric compression, is first seen in the onset image and is identified by red arrows in the images after the substorm onsets. (Note that resolution is poor near the edge of the imager field-of-view, which affects the images for the second onset at 15–18 MLT. However, the brightening in this region is clear). Expansion of the substorm auroral bulge can be seen in images after the onset, as can further brightening of the compressional auroral enhancement. Merger of the two responses can be seen in the final images for each event, brightened auroral extending over ~16 hr in MLT for the first event and ~14 hrs of MLT for the second event. Based on the solar wind, geosynchronous particle, ground H, and auroral observations, it is clear that impact of the P_{dyn} increases occurred at the onset of both of these large, substorm-related disturbances.

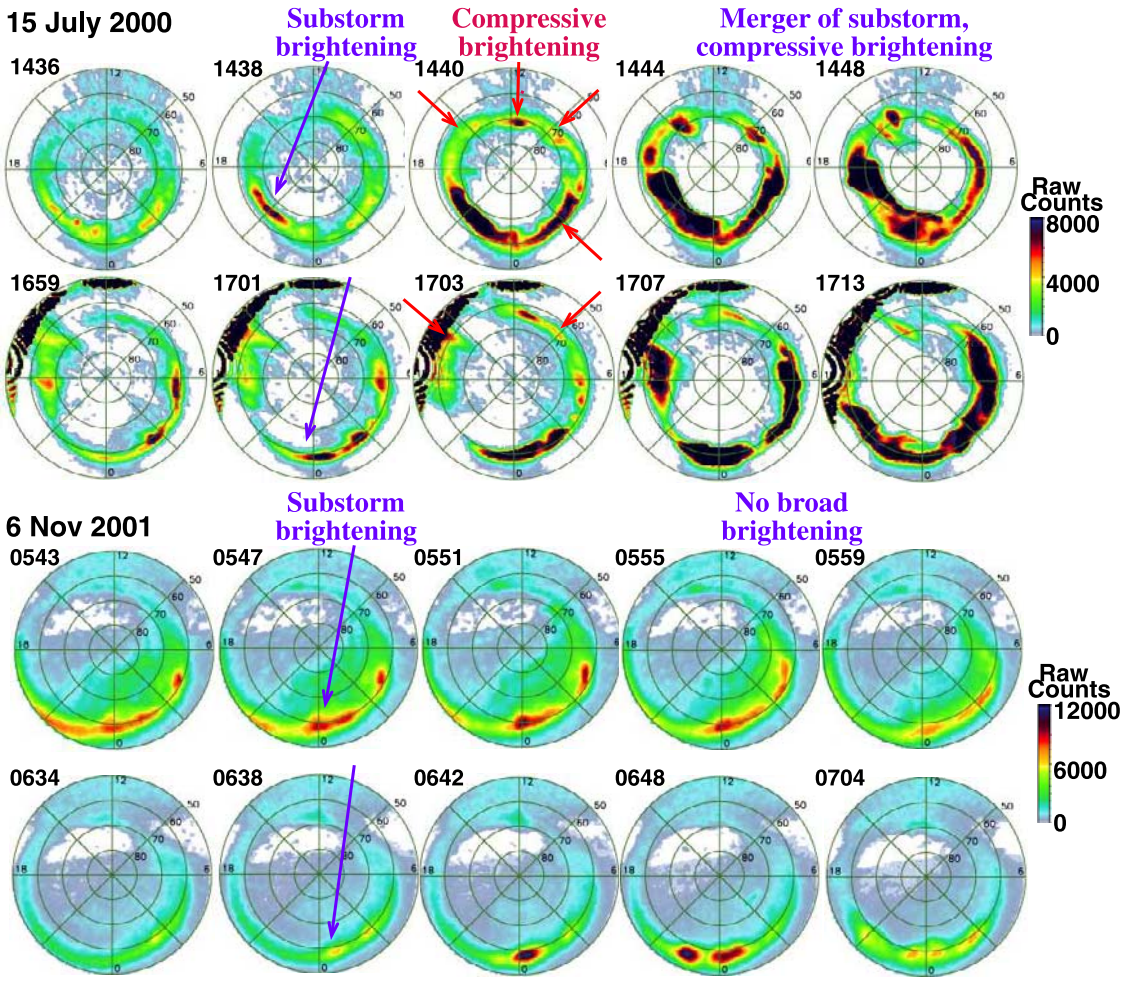

Figure 3. Upper two rows show selected WIC images for the two disturbances identified by vertical dashed lines in Figures 1 and 2. The bottom two rows show selected images for the two disturbances identified by vertical dashed lines in Figure 3. Midnight is at the bottom and dusk is to the left of each image. Circles are shown at 10° magnetic latitude intervals.

[10] Figure 4 shows IMF and solar wind measurements, AMIE AL and Sym-H indices from 0–8 UT on 6 November 2001. The Geotail data were obtained within the dawn side magnetosheath, and the IMF is shown multiplied by 0.5 in order to facilitate comparison with the IMF from ACE within the solar wind. The ACE data have been linearly time-shifted based on the Geotail magnetic fields. As with the previous event, because of high particle backgrounds, the ACE broad-energy-range plasma data with temporal resolution of ~30 minutes has been used to fill data gaps during the time interval of interest. Since Geotail was within the magnetosheath at this time, its plasma observations cannot be used to approximate solar wind conditions. The storm sudden commencement occurred at ~0151 UT and a strong storm main phase initiated immediately thereafter, Sym-H reaching ~−250 nT in ~15 min due to the very strong southward IMF. WIC observations are available for the two strong IMF northward turnings identified by vertical dashed lines in Figure 4. These northward turnings were accompanied by significant reductions in $|B_y|$ and would be expected to trigger a nightside substorm. While high time-resolution plasma measurements in the solar wind are not available, the dayside ground H and dayside geosynchronous protons in the bottom three panels of Figure 4 do not show signatures of P_{dyn} increases impacting the magnetosphere near the times of the two identified northward turnings. These two events are the only examples during the large storms considered here where we would expect a substorm from the IMF change, but the IMF change appears to not have been accompanied by an increase in P_{dyn}. Note that the ground H on the nightside (station FFN in Figure 4) shows positive H increases indicating formation of the substorm current wedge. Energetic particle data near midnight is not available from the LANL spacecraft for these events, but Goes 8 and 10 magnetic fields (not shown), respectively, show nightside magnetic field dipolarization for the two events. Also, unlike for the P_{dyn} increase events, further depressions of AL were not seen for these events. This is not unexpected since AL was already strongly depressed before the evens, which is an expected result of the strongly southward IMF driving quite strong convection before the event onsets.

[11] WIC images for the above two disturbances on 6 November are shown in the bottom two rows, respectively,

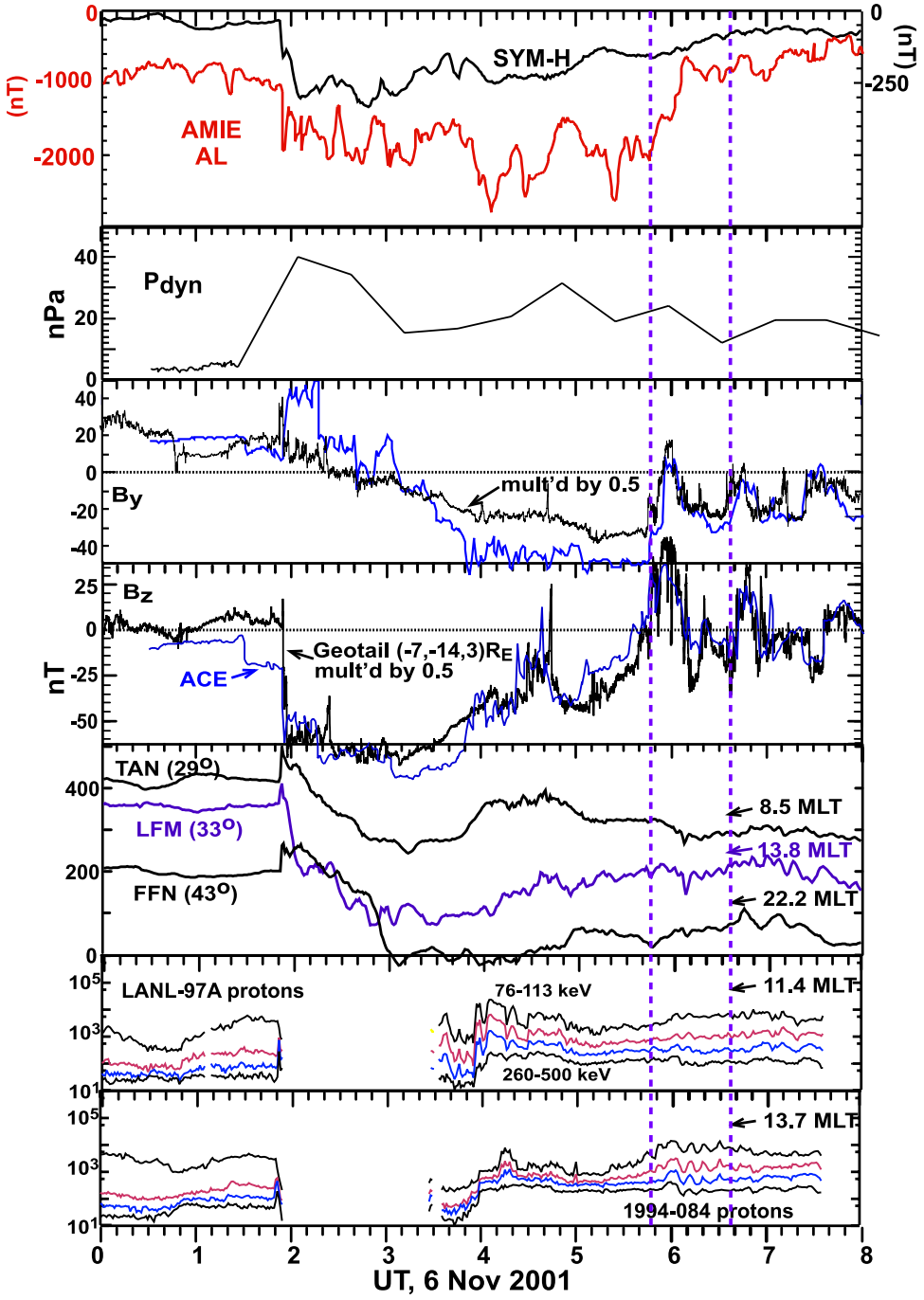

Figure 4. IMF and solar wind measurements, AMIE AL and Sym-H indices from 0–8 UT on 6 November 2001. The Geotail data were obtained within the dawn side magnetosheath, and the IMF is shown multiplied by 0.5 in order to facilitate comparison with the IMF from ACE within the solar wind. The ACE data have been linearly time-shifted based on the Geotail magnetic fields. The ACE re-analyzed low-time-resolution broad-energy-range plasma data is shown in the second panel because the normal level 2 data is not available during this period. Mid-latitude ground H observations from two dayside stations and one nightside station chosen to be near dawn, noon, and dusk and energetic proton fluxes from two dayside LANL spacecraft are shown in the bottom three panels. Vertical dashed lines indicate the times of the two disturbances discussed in the text.

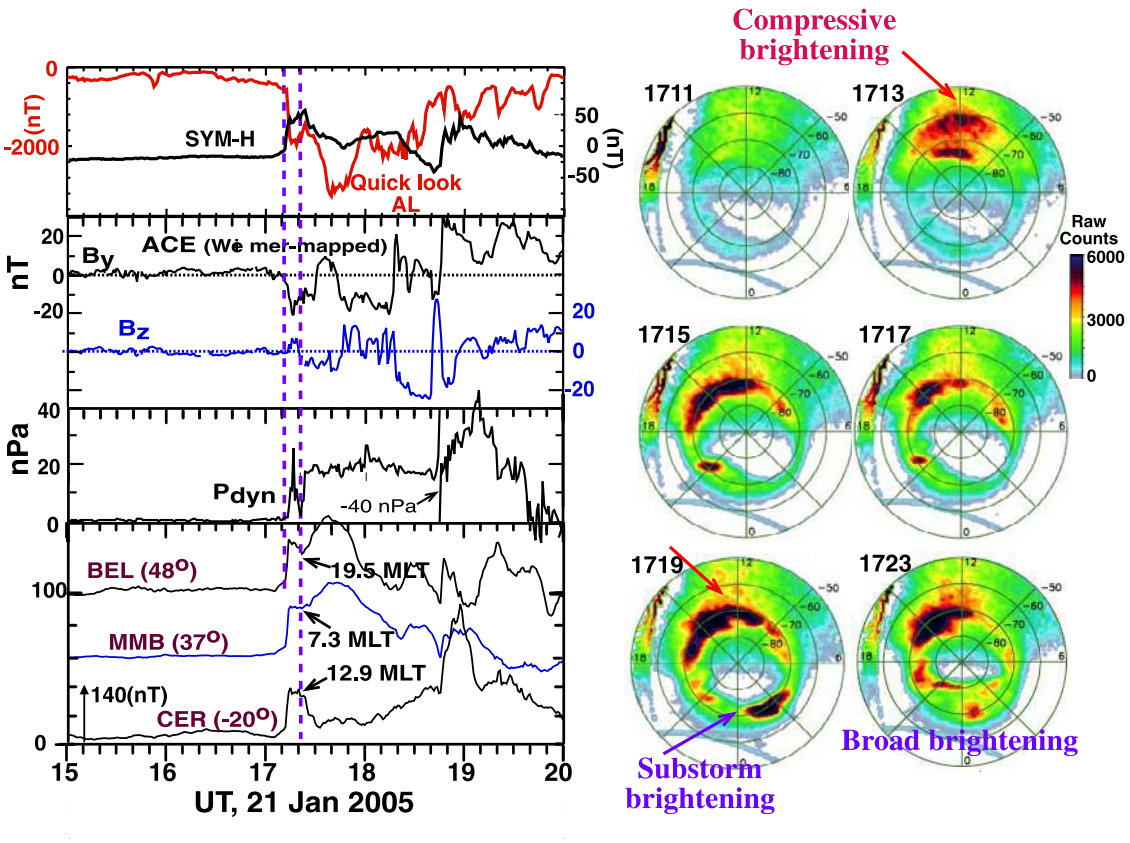

Figure 5a. Interplanetary, ground H, Sym-H, AL, and WIC images on 21 January 2005. Vertical dashed lines indicate the times of the two disturbances discussed in the text.

of Figure 3. Again successive 2 min images are shown for the times before, at, and after the first discernible auroral intensification, along with two later expansion phase images that show the subsequent auroral development. These images show important differences from what occurred for the two disturbances on July 15 that included a P_{dyn} increase. A nightside substorm auroral brightening is seen near midnight for both events. However, there is no evidence for brightening away from the substorm onset region, as expected due to the lack of magnetospheric compression. Expansion of the substorm auroral bulge can be seen in images after the onset, but very broad auroral disturbances, as seen for the 15 July events, do not occur. This difference between substorms triggered by IMF changes and those triggered by P_{dyn} increases is consistent with that found by *Lyons et al.* [2005], though the P_{dyn} increase events included here have an IMF change that would be expected to have triggered a substorm while the events considered by *Lyons et al.* [2005] had only P_{dyn} triggers.

[12] The observations in Figures 1–4 suggest that the impact on the magnetosphere of a significant P_{dyn} increase can lead to broad, strong storm disturbances, and that the broad, intense response is due to the combination of the substorm and compressional effects on the magnetosphere. During the storms considered here, there are WIC images for three additional stormtime disturbances. Interplanetary, ground H, Sym-H, AL, and WIC images for these disturbances are shown in Figures 5a–5c. Two very large pressure impacts occurred close together at 1712 and 1720 UT on 21 January 2005 that brought P_{dyn} from ~2 nPa to ~20 nPa. Both P_{dyn} increases can be seen in the Weimer-mapped ACE observations and the dayside ground H observations in Figure 5a, and in the LANL geosynchronous energetic particle observations (not shown). AL dropped dramatically for both increases, and both can be seen as dayside auroral enhancements in the WIC images at 1713 and 1719 UT shown in Figure 5a. There was not significant southward IMF B_z or large IMF $|B_y|$ prior to the first impact, and a substorm auroral brightening was not seen. There was a several minutes period of large IMF $|B_y|$ prior to the second impact, and a nightside substorm onset can be seen in the 1719 UT image, leading to a global auroral brightening that shows clearly in the 1723UT image.

[13] Two large increases that brought P_{dyn} to ~40 nPa in two steps occurred near 0600 and 0608 UT during the 15 May 2005 storm (see Figure 5b). As for the 21 January event, both P_{dyn} increases can be seen in the Weimer-mapped ACE observations and dayside ground H observations in Figure 5b and in the LANL geosynchronous energetic particle observations (not shown). Both increases can be seen as dayside auroral enhancements in the WIC images at 0601 and 0607 UT shown in Figure 5b. A quite weak nightside substorm onset can be seen in the WIC image in association with the first pressure impact, and a stronger onset, leading to a broad auroral disturbance, can be seen following the second onset.

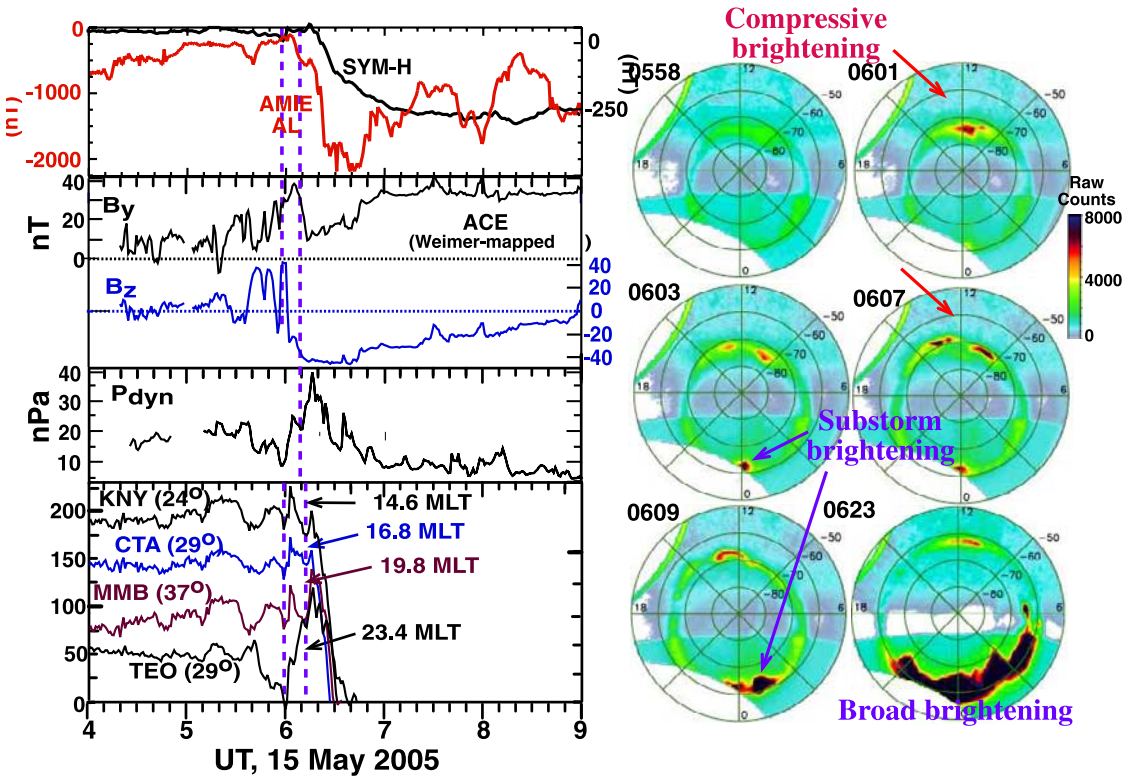

Figure 5b. Interplanetary, ground H, Sym-H, AL, and WIC images on 15 May 2005. Vertical dashed lines indicate the times of the two disturbances discussed in the text.

[14] An interesting feature of the above disturbances is the unusually short growth phase before the onsets of substorm disturbances. There was ~8 min of strongly enhanced $|B_y|$ prior to the 1720 UT onset on 21 Jan 2005, and there was strongly negative B_z and extremely large $|B_y|$ for ~8 min prior to the 0608 UT onset on 15 May. What gave rise to the growth phase before the earlier very weak onset on May 15 is not clear. These observations suggest that a substantially shorter than typical growth phase may be sufficient for there to be a substorm onset if the IMF $|B_y|$ or negative Bz prior to the pressure increase and/or the pressure increase is unusually large.

[15] Two pressure increases ~33 min apart during the 24 August 2005 storm are identified in Figure 5c. Responses are the same as for the previous events with the exception of the strong decrease, rather than an increase, in dayside H associated with the second pressure impact. Such a decrease has been shown to occur when a P_{dyn} enhancement intensifies an already strong partial ring current and its closure currents [*Shi et al.*, 2006], and, unlike for the previously discussed P_{dyn} increase events, this event occurred during the storm main phase after Sym-H had decreased to ~−75 nT.

3. Disturbances During Sawtooth-Event Storms

[16] In the previous section, we discussed five examples during major magnetic storms that indicate that impact of a substantial P_{dyn} increase at the time of a disturbance onset, and the resulting two-mode (compressional and substorm) response, leads to unusually large-scale auroral disturbances. Most of the events occurred during the initial storm phase, prior to the development of the storm main phase, when P_{dyn} is often large and variable. Storms that have been referred to as sawtooth events are generally more moderate than the above storms. We consider here storms that occurred on 11 August 2000, 4 October 2000, 14 October 2000, 22 October, 2001, 18 April 2002, and 2 August, 2002, the minimum Sym-H on these storm days being, respectively, −108, −141, −101, −167, −121, and −115 nT. These storms all have a series of large disturbances occurring ~2–4 hrs apart, most of which occurred after the storm main phase and while Sym-H was depressed.

[17] Solar wind and geosynchronous energetic electron observations from the storm on 22 October 2001 are shown in Figure 6. As can be seen in the top panel, Sym-H remained near −125 nT throughout the period shown. Solar wind data are available from three spacecraft for this storm and are shown as Weimer-mapped to X_{GSM} = 17 R_E. Both WIND and Geotail were quite nearby the Earth's magnetosphere, and the IMF measurements from the three spacecraft agree unusually well with each other. Thus it is likely that the measurements quite well represent the IMF that impacted the magnetosphere. The P_{dyn} variations are larger as measured by Geotail than as measured by ACE and WIND, but the times of the major increases and decreases agree quite well between the three spacecraft. The energetic electron measurements in Figure 6 are from two of four available LANL spacecraft, having been selected to be ~12 hr in MLT apart, orange and dark blue thick vertical lines

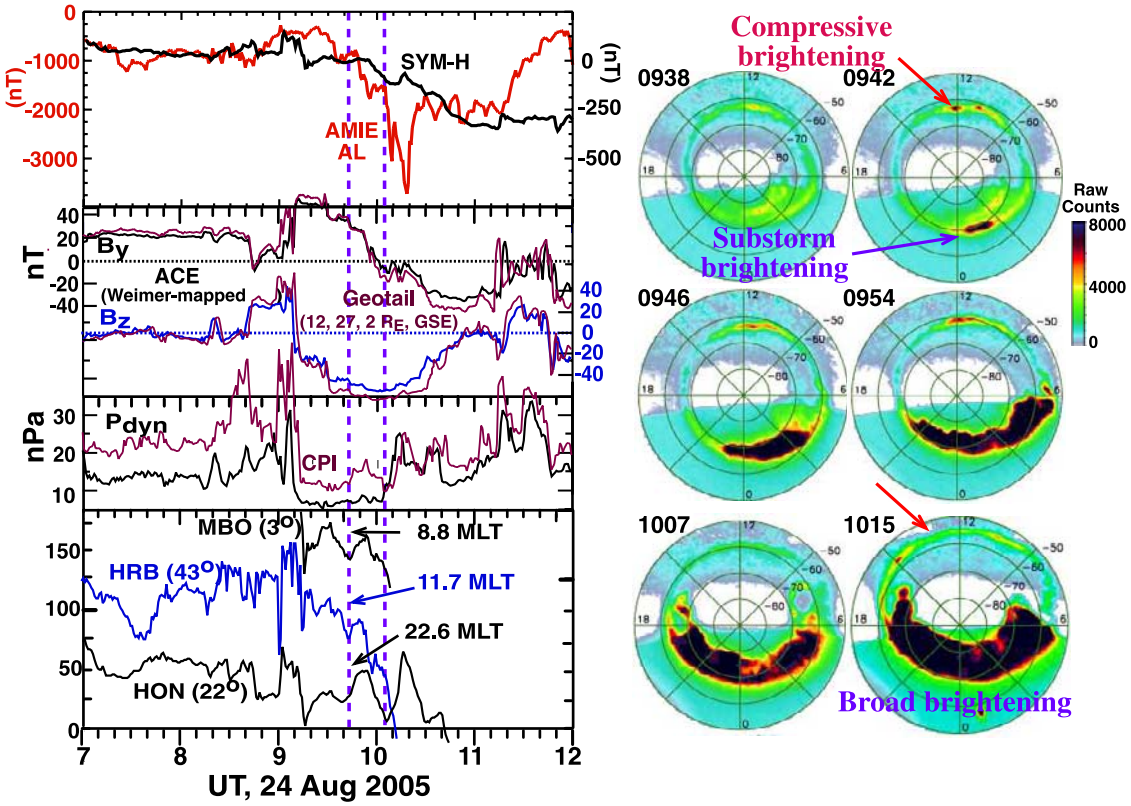

Figure 5c. Interplanetary, ground H, Sym-H, AL, and WIC images on 24 August 2005. Vertical dashed lines indicate the times of the two disturbances discussed in the text.

identifying 12 and 24 MLT, respectively. Dashed vertical magenta lines identify onsets that lead to the larger and more prolonged geosynchronous particle enhancements, which are often referred to as the "teeth" of sawtooth events. There were substantial drops in AL associated with each of these disturbances, except for the one near 16 UT. However, the values of AL were weaker than seen for most of the strong storm disturbances, suggesting that these events are somewhat weaker. The first and last of these disturbances are associated with IMF northward turnings that are known to trigger substorms [*Lyons et al.*, 1997; *Hsu and McPherron*, 2002] and have approximately constant P_{dyn}. (Short <10 min variations, such as the increase in P_{dyn} that was observed by Geotail near the time of the last disturbance are not considered here. This increase was smaller and even shorter as observed by WIND, and the low latitude H data do not show evidence for a significant or prolonged increase at this time.)

[18] A substantial increase in P_{dyn} is observed near the time of onset for 3 (at 1345, 1556, and 1810 UT) of the remaining 4 disturbances. The structure of P_{dyn} is somewhat different between the three spacecraft for the 1103 UT onset, so that the precise structure of the P_{dyn} variations that impacted the magnetosphere near this time is not clear from the spacecraft observations. Also, the P_{dyn} increase is seen in the solar wind data a few minutes after onset of the 1556 UT disturbance, though this time difference is well within the expected errors of the Weimer mappings. To determine the precise time of the pressure impacts, we examined other data. Ground H data from the near noon region are shown in the bottom panel of Figure 6 from four stations selected so that one station is near noon for each disturbance. These data show positive H perturbations at the time of onset for the 3 disturbances for which a P_{dyn} increase was clearly observed within the solar wind, including the onset of the disturbance near 16 UT, thus verifying the impact of a P_{dyn} increase at these times. A positive H perturbation is also seen at the onset of the 1103 UT disturbance, indicating that a P_{dyn} increase impacted the magnetosphere at this time as well. The energetic electrons show responses at the time of onsets at both spacecraft for all 4 of these disturbances, the response on the spacecraft nearest noon also giving additional evidence that there was an impact of a P_{dyn} increase at these times. This near-noon response (an abrupt decrease) is clear in the LANL01 electron fluxes for the 1103 UT onset. These four disturbances all also had an IMF Bz or By change that would have been expected to trigger a substorm independent of the P_{dyn} increase. Note that signatures of a P_{dyn} increase are not seen in the dayside geosynchronous and ground H observations from the first and last onsets on 22 October.

[19] Figure 7 shows WIC images for the 1345 UT disturbance that, based on the interplanetary, ground H, and geosynchronous electron measurements, was triggered in part by a P_{dyn} increase, and for the 2156 UT tooth that, based on the interplanetary and ground H measurements, was triggered primarily by the IMF and did not have a concurrent P_{dyn} increase lasting more than 10 min. As for

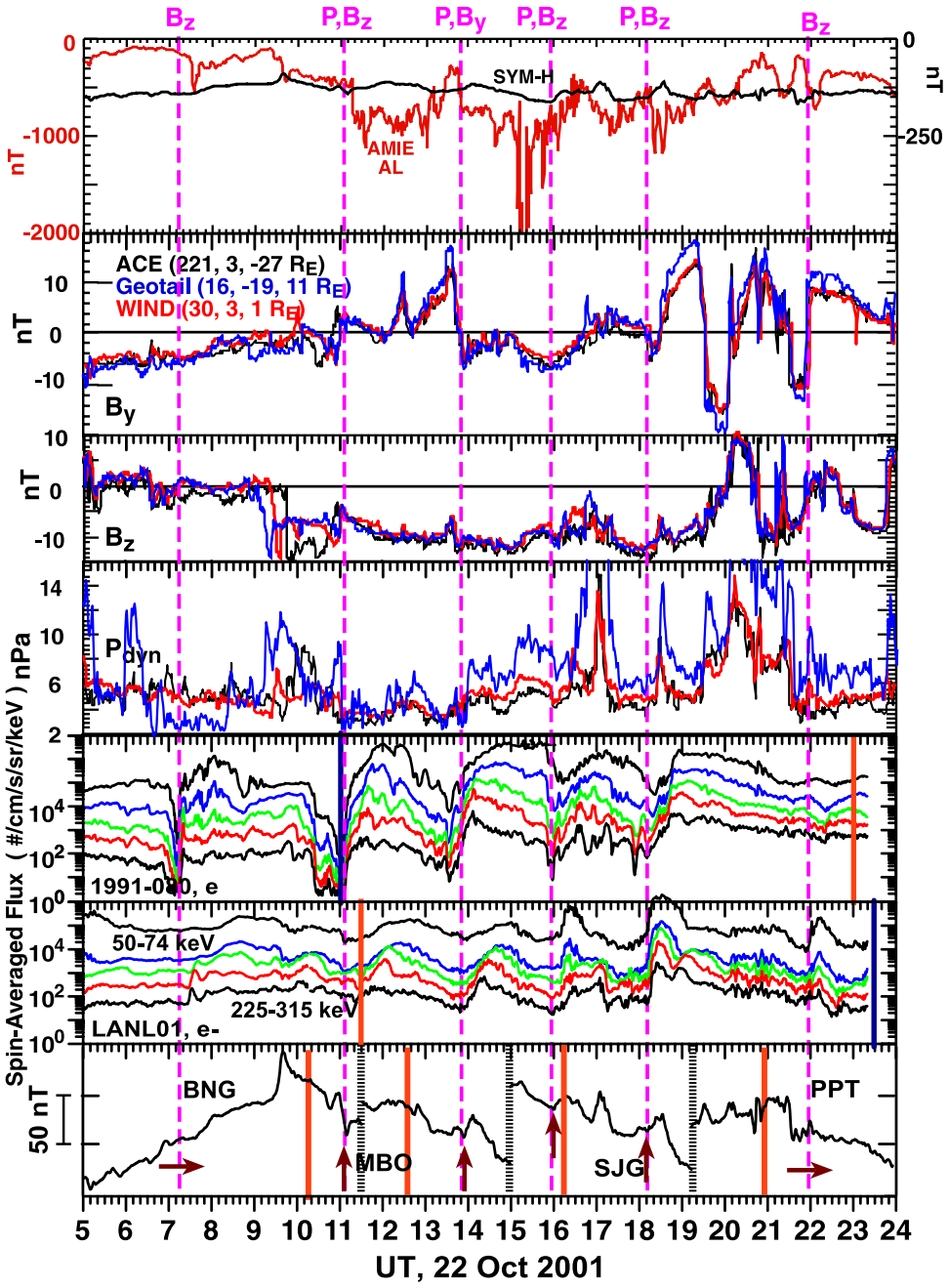

Figure 6. Solar wind plasma, IMF, Sym-H, AL, and geosynchronous energetic electron observations for 22 October 2001. The solar wind data are shown as mapped to $X_{GSM} = 17\ R_E$ directly in front of the magnetosphere using the *Weimer et al.* [2003] technique. Spacecraft locations in GSM at the midpoint of the time interval shown are indicated. Energetic electron observations are from two of the four available LANL spacecraft, orange and dark blue thick vertical lines identifying 12 and 24 MLT, respectively. Fluxes are from five energy channels ranging from 50–74 keV to 225–315 keV. Dashed vertical magenta lines identify major disturbance onsets.

the events discussed earlier, images, which are available every two minutes, have been selected to illustrate the temporal evolution of the auroral enhancements for each disturbance. It can be seen that there are very significant differences in the auroral evolution of the two disturbances, and the differences are consistent with those discussed above for the disturbances during large storms. The IMF triggered tooth shows only the nightside auroral brightening, which is followed by azimuthal expansion of bright aurora over a few hours in MLT. There is no other persistent brightening during this period of expansion of the bright aurora. This is the ordinary substorm response, without anything else. Recovery of the aurora then starts ~10–12 min after onset. The pressure event has the two-mode response, with both the compressive auroral enhancement on the dayside and the nightside substorm

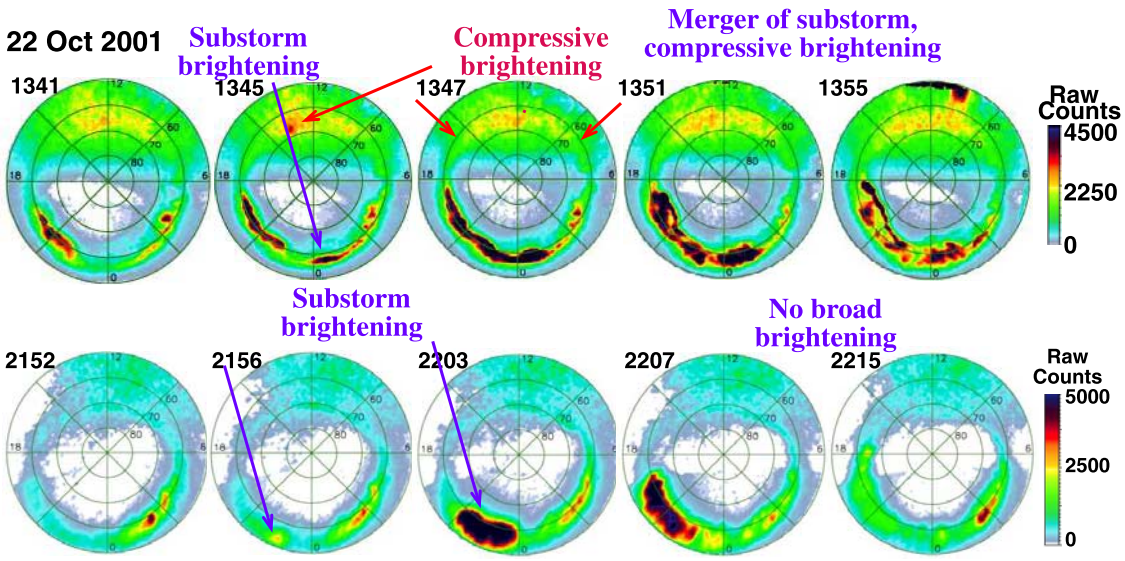

Figure 7. WIC images for the 1345 UT and 2156 UT disturbances identified in Figure 6.

enhancement initiating near the time of onset. The pressure enhancement was not as great as for some of the disturbances during major storms, so that the dayside auroral enhancement was not large. However enhancement of the aurora from ~7 to 17 MLT can be seen. Within 10 min of onset, the region of enhanced aurora on the nightside broadened to cover ~9 hr of MLT, which then extended to cover ~12 hrs in MLT in later images (not shown). Also, the decay of the enhanced emissions is far less within ~20–25 min than for IMF substorms.

[20] There were also WIC images available (not shown) for the 0715 UT IMF triggered disturbance and the 1103 UT disturbance that was associated with a P_{dyn} increase. Only a nightside auroral brightening is seen for the 0715 UT tooth, consistent with this being an IMF substorm, and the nightside auroral brightening extended to cover ~5 hrs of MLT. A nightside brightening is also seen for the 1103 UT tooth, but the effects of compression from a pressure impact cannot be unambiguously identified near the time of onset in the dayside aurora. However, the region of enhanced aurora on the nightside broadened to cover ~10 hr of MLT, consistent with what is seen for the other disturbances discussed here that occurred as a result of a P_{dyn} increase. Thus for these 4 disturbances, we see that the auroral disturbances became much broader for the disturbances that were associated with a P_{dyn} increase than for the disturbances that were not, consistent with what we found during the intense storms.

Table 1. Y (Yes) and N (No) Identifies Whether or Not Evidence for a P_{dyn} Increase at the Time of Onset is Seen for Each Disturbance in the Solar Wind (Wind), the Dayside WIC Aurora (WIC), the Dayside Ground H (Day H), and the Dayside Geosynchronous Electrons (Geo Elec)[a]

Date	Onset UT	Wind	WIC	Day H	Geo elec	P_{dyn} evidence	Bright, hr
11 Aug 2000	415	Y	Y	Y	Y	Y	9
11 Aug 2000	639	N	N	N	N	N	7
11 Aug 2000	820	N	N	N	N	N	6
11 Aug 2000	1030	N	N	N	N	N	7
4 Oct 2000	611	N	N	N	N	N	6
4 Oct 2000	933	N	N	N	Y	N	5
4 Oct 2000	1706	Y	N	Y	Y	Y	9
4 Oct 2000	1959	N	N	Y	Y	Y	8
4 Oct 2000	2132	N	Y	Y	Y	Y	7
14 Oct 2000	655	Y	N	Y	Y	Y	13
14 Oct 2000	954	Y	Y	Y		Y	14
22 Oct 2001	715	N	N	N	N	N	5
22 Oct 2001	1103	N	N	Y	Y	Y	10
22 Oct 2001	1345	Y	Y	Y	Y	Y	13
22 Oct 2001	2156	N	N	N	N	N	5
18 Apr 2002	313	N	Y	Y		Y	14
18 Apr 2002	531	Y	N	N	Y	Y	14
18 Apr 2002	808	Y	Y	Y	Y	Y	13
18 Apr 2002	1133	Y	Y	Y	Y	Y	10
18 Apr 2002	2102	Y	N	Y	Y	Y	10

[a] P_{dyn} evidence identifies whether or not two of the preceding show evidence of a P_{dyn} increase at onset. Bright (hr) gives the maximum MLT range of enhanced aurora during each disturbance.

[21] Table 1 summarizes what we found for all major disturbances during the above moderate storms for which there was useable global auroral coverage from WIC. (Observations showing the effect of pressure impacts for many of these disturbances can be found in *Lee et al.* [2004] (14 October 2000, 18 April 2002, and 20 August 2002 storms), in *Lyons et al.* [2005] (11 August 2000, 14 October 2000, and 18 April 2002 storms), and in *Lee et al.* [2005] (11 August 2000, 4 October 2000, and 14 October 2000 storms). Columns 3–6, respectively, identify whether or not evidence for a P_{dyn} increase at the time of onset is seen for each disturbance in the solar wind, the dayside aurora observed by WIC, the dayside ground H, and the dayside geosynchronous electrons (there is no entry if geosynchronous electron observations on the dayside were not available). If evidence is seen in two or more of these, then we identify in column 7, (labeled P_{dyn} evidence) that there is substantial evidence of a P_{dyn} increase at onset. There are fourteen such disturbances. Column 7 also identifies those cases for which such evidence does not exist. There are seven such disturbances, and evidence for a P_{dyn} increase is not seen in any of the observations for all but one of them. We thus have reasonable confidence in the determination that a substantial P_{dyn} increase did not impact the magnetosphere for these disturbances. There is somewhat more uncertainty about the existence of a P_{dyn} increase for the other 14 disturbances because evidence for a P_{dyn} increase is not seen in all the observations for many of the disturbances. For example, a P_{dyn} increase was not observed by the available interplanetary spacecraft for five of these fourteen disturbances, though this is a reasonable result of the difficulties of mapping interplanetary features from an observing spacecraft to the magnetosphere. However, by requiring that there be evidence for a P_{dyn} increase in a last two of the sets of observations, it is reasonable that most of these identifications are correct.

[22] The last column in Table 1 gives the maximum MLT range of enhanced aurora during each disturbance. These ranges are 5–7 hrs for the disturbances without evidence for a P_{dyn} increase at onsets, but are 7–15 hrs with a median of 11 to 12 hr for the disturbances having evidence for a P_{dyn} increase. This provides support for the role of P_{dyn} increases in creating unusually broad disturbances and that other substorm disturbances are generally not as broad.

4. Conclusions

[23] We have combined interplanetary observations, global auroral images from the WIC imager, geosynchronous energetic electrons observations, and mid/low-latitude dayside ground H observations for 7 large storm associated disturbances and 21 disturbances during storms that have been referred to as sawtooth events by the community, because of large disturbances occurring every ~2–4 hrs. Evidence for a substantial P_{dyn} increase at onset was found for 19 of these 28 disturbances. We found that, on the average, auroral brightenings extended over about twice as broad an MLT range for these 19 disturbances than did the auroral brightenings for the disturbances without evidence for a P_{dyn} increase at onset. This indicates that P_{dyn} increases at onset contribute to the broadening of large-scale aurora disturbances that often occurs during magnetic storms. Our results indicate that it is the combination of the global compression response to a P_{dyn} increase and the nightside substorm response that gives a much broader auroral response for many stormtime disturbances than is seen for other substorm disturbances.

[24] A greater than 7 hr wide region of enhanced aurora was not seen for any of the 9 disturbances studied here that we did not associate with evidence for a P_{dyn} increase. However, it is possible that, under the proper circumstances, other auroral disturbances driven by magnetospheric processes might also contribute to the MLT-extent of the auroral oval emissions during active times, an area that warrants further investigation. We also found some evidence that a substantially shorter than typical growth phase may be sufficient for there to be a triggered substorm onset under storm conditions if the preceding IMF $|B_y|$ or negative Bz, and/or a pressure increase at onset, is unusually large. This possibility also warrants further study.

[25] **Acknowledgments.** This research was supported at UCLA in part by NSF grants ARC-0611717 and ATM-0646233, NASA grant NNG05GF29G. The work at Chungbuk National University was supported by Grant No. R01-2007-000-10674-0 from the Korea Science and Engineering Foundation. We are grateful to Harald Frey for assistance in understanding the analysis of the WIC images, to Thomas Immel for his help in getting the FUV imager software running at UCLA, to W. R. Paterson for assistance in validating the Geotail CPI solar wind data, and to G. D. Reeves for supplying the LANL energetic particle data and for helpful comments. We also thank Aaron Ridley and Xia Cai for running AMIE and providing us with AL index obtained from their runs. The solar wind plasma and magnetic field data of ACE, Wind, and Geotail used here were obtained from NASA's CDAWeb site, and we are grateful to each of the principal investigators, D.J. McComas, N. Ness, K. Ogilvie, R. Lepping, L. Frank, and S. Kokubun. In cases where standard level 2 ACE SWEPAM data had gaps, re-analysis of lower resolution data to verify original observations or fill the data gaps was provided courtesy of Ruth Skoug and the SWEPAM team at Los Alamos National Laboratory under the auspices of the US Department of Energy, and at Southwest Research Institute with funding through the NASA ACE program. The geomagnetic data used were obtained from the World Data Center for Geomagnetism, Kyoto.

[26] Amitava Bhattacharjee thanks Finn Soraas and James Wanliss for their assistance in evaluating this paper.

References

Elphinstone, R. D., J. S. Murphree, and L. L. Cogger (1996), What is a global auroral substorm, *Rev. Geophys.*, *34*, 169.

Henderson, M. G., G. D. Reeves, R. Skoug, M. T. Thomsen, M. H. Denton, S. B. Mende, T. J. Immel, P. C. Brandt, and H. J. Singer (2006), Magnetospheric and auroral activity during the 18 April 2002 sawtooth event, *J. Geophys. Res.*, *111*, A01S90, doi:10.1029/2005JA011111.

Hsu, T.-S., and R. L. McPherron (2002), An evaluation of the statistical significance of the association between northward turnings of the interplanetary magnetic field and substorm expansion onsets, *J. Geophys. Res.*, *107*(A11), 1398, doi:10.1029/2000JA000125.

Lee, D.-Y., L. R. Lyons, and K. Yumoto (2004), Sawtooth oscillations directly driven by solar wind dynamic pressure enhancements, *J. Geophys. Res.*, *109*, A04202, doi:10.1029/2003JA010246.

Lee, D.-Y., L. R. Lyons, and G. D. Reeves (2005), Comparison of geosynchronous energetic particle flux responses to solar wind dynamic pressure enhancements and substorms, *J. Geophys. Res.*, *110*, A09213, doi:10.1029/2005JA011091.

Lyons, L. R., G. T. Blanchard, J. C. Samson, R. P. Lepping, T. Yamamoto, and T. Moretto (1997), Coordinated observations demonstrating external substorm triggering, *J. Geophys. Res.*, *102*, 27,039.

Lyons, L. R., D.-Y. Lee, C.-P. Wang, and S. B. Mende (2005), Global auroral responses to abrupt solar wind changes: Dynamic pressure, substorm, and null events, *J. Geophys. Res.*, *110*, A08208, doi:10.1029/2005JA011089.

Reeves, G. D., et al. (2002), Global "sawtooth" activity in the April 2002 geomagnetic storm, *Eos Trans. AGU*, *83*(74), Fall Meet. Suppl., Abstract SA12A-05.

Reeves, G. D., et al. (2004), IMAGE, POLAR, and geosynchronous observations of substorms and ring current ion injection, in *Disturbances in*

Geospace: The Storm-Substorm Relationship, *Geophys. Monogr. Ser.*, vol. 142, edited by A. S. Sharma et al., pp. 89–100, AGU, Washington, D. C.

Richmond, A. D. (1992), Assimilative mapping of ionospheric electrodynamics, *Adv. Space Res.*, *6*, 59.

Shi, Y., E. Zesta, L. R. Lyons, K. Yumoto, and K. Kitamura (2006), Statistical study of effect of solar wind dynamic pressure enhancements on dawn-to-dusk ring current asymmetry, *J. Geophys. Res.*, *111*, A10216, doi:10.1029/2005JA011532.

Smith, C. W., et al. (2001), ACE Observations of the Bastille day 2000 interplanetary disturbances, *Solar Phys.*, *204*, 229–254.

Wanliss, J. A., and K. M. Showalter (2006), High-resolution global storm index: Dst versus SYM-H, *J. Geophys. Res.*, *111*, A02202, doi:10.1029/2005JA011034.

Weimer, D. R. (2004), Correction to "Predicting interplanetary magnetic field (IMF) propagation delay times using the minimum variance technique", *J. Geophys. Res.*, *109*, A12104, doi:10.1029/2004JA010691.

Weimer, D. R., D. M. Ober, N. C. Maynard, M. R. Collier, D. J. McComas, N. F. Ness, C. W. Smith, and J. Watermann (2003), Predicting interplanetary magnetic field (IMF) propagation delay times using the minimum variance technique, *J. Geophys. Res.*, *108*(A1), 1026, doi:10.1029/2002JA009405.

J. U. Kozyra, Space Physics Research Laboratory, University of Michigan, 2455 Hayward Street, Ann Arbor, MI 48109, USA. (jukozyra@umich.edu)

D.-Y. Lee, Department of Astronomy and Space Science, Chungbuk National University, 410 Sungbong-Ro, Heungduk-gu, Cheongju, Chungbuk 361-763, South Korea. (dylee@chungbuk.ac.kr)

L. R. Lyons, C.-P. Wang, and S. Zou, Department of Atmospheric and Oceanic Sciences, University of California, Los Angeles, 405 Hilgard Avenue, Los Angeles, CA 90095-1565, USA. (larry@atmos.ucla.edu; cat@atmos.ucla.edu; sha@atmos.ucla.edu)

S. B. Mende, Space Sciences Laboratory, University of California, 7 Gauss Way, Berkeley, CA 94720-7450, USA. (mende@ssl.berkeley.edu)

J. M. Weygand, Department of Earth and Space Sciences, University of California, Los Angeles, 405 Hilgard Avenue, Los Angeles, CA 90095-1565, USA. (jweygand@igpp.ucla.edu)